MicroRNA Detection

International Edition: DOI: 10.1002/anie.201504887
German Edition: DOI: 10.1002/ange.201504887

A Rapid, Amplification-Free, and Sensitive Diagnostic Assay for Single-Step Multiplexed Fluorescence Detection of MicroRNA

*Zongwen Jin, Daniel Geißler, Xue Qiu, K. David Wegner, and Niko Hildebrandt**

Dedicated to Hans-Gerd Löhmannsröben on the occasion of his 60th birthday

Abstract: *The importance of microRNA (miRNA) dysregulation for the development and progression of diseases and the discovery of stable miRNAs in peripheral blood have made these short-sequence nucleic acids next-generation biomarkers. Here we present a fully homogeneous multiplexed miRNA FRET assay that combines careful biophotonic design with various RNA hybridization and ligation steps. The single-step, single-temperature, and amplification-free assay provides a unique combination of performance parameters compared to state-of-the-art miRNA detection technologies. Precise multiplexed quantification of miRNA-20a, -20b, and -21 at concentrations between 0.05 and 0.5 nM in a single 150 μL sample and detection limits between 0.2 and 0.9 nM in 7.5 μL serum samples demonstrate the feasibility of both high-throughput and point-of-care clinical diagnostics.*

More than half of the human genes are regulated by microRNAs (miRNAs) and one type of miRNA can have several hundreds of target genes.[1–3] Due to their importance in disease development, miRNAs have become next-generation biomarkers for diagnosis and prognosis.[4–6] This has led to a strong demand for routine quantitative detection of miRNA dysregulations in cells, tissues, and blood.[7,8] Two of the main disadvantages for the development of specific and sensitive detection technologies for miRNA are their short lengths (19 to 25 nucleotides) and strong sequence similarities that must be distinguishable in complex samples, which contain many different miRNAs (and precursor miRNAs) at different concentrations. Large differences in melting temperatures due to the sequence variability among miRNAs have made hybridization-based capturing probes difficult to apply for large-scale expression profiling.[9] On the other hand practical issues of preamplification in clinical setups, the requirement of miRNA labeling or indirect amplification, and complementary DNA conversion steps (often the primary cause of variations) are among the main problems for establishing polymerase chain reaction (PCR)-based technologies as robust and reproducible tools for real-life clinical diagnostics.[10,11] Problems with the biofouling of solid supports, low throughput, difficulties in upscaling or miniaturization, time-consuming and labor-intensive preparation and separation steps, and sophisticated and expensive analysis are further problems that can limit the application in clinical diagnostics.

An overview of the many miRNA detection technologies and their performance parameters concerning diagnostic applications are presented in Table 1 A. The large technological versatility and the importance of specific requirements for different sample conditions and diagnostic purposes illustrate the fact that a perfect miRNA detection technology does not exist. Although quantitative reverse transcription polymerase chain reaction (qRT-PCR) can provide sensitivity down to a few miRNA copies and microarrays allow parallel detection of many different miRNAs, new technological developments that combine ease of use, rapid preparation, detection, and analysis, multiplexed detection, and high sensitivity to answer the increasing demand of miRNA clinical diagnostics are not available today. Moreover, it would be very beneficial if such a technology could be easily transferred to other nucleic acid based biomarkers, such as sequence-specific DNA targets, which play an important role in the diagnosis and therapy of genetic diseases,[12] typing and tracing sources of infectious agents,[13] forensics,[14] and the detection of single-nucleotide polymorphisms (SNPs) of ancient DNAs.[15] Our fluorescence assay affords a unique combination of diagnostic performance parameters (Table 1 B) by careful implementation of several spectroscopy technologies (FRET, time-gated fluorescence detection, color multiplexing, biospectral crosstalk correction) into a versatile nucleic acid assay design using different hybridization and ligation steps.

The optical detection is based on time-gated Förster resonance energy transfer (TG-FRET)[16] from the luminescent terbium complex Lumi4-Tb (Tb)[17] to different organic dyes (Cy3.5, Cy5, and Cy5.5). Tb has four bright and narrow photoluminescence (PL) emission bands, which overlap with the absorbance spectra of all three different dyes (Figure 1 a,b). Förster distances were 6.5 nm, 6.3 nm, and 5.7 nm for Tb–Cy3.5, Tb–Cy5, and Tb–Cy5.5, respectively. This single-donor/multiple-acceptors approach allowed triplexed Tb-to-dye FRET. To overcome Tb PL into the dye detection channels as well as between the different dye channels (Figure 1 b) we used our recently developed correction method for immunoassays,[18] which we adapted to multiplexed miRNA detection (vide infra).

[*] Dr. Z. Jin, X. Qiu, Dr. K. D. Wegner, Prof.Dr. N. Hildebrandt
NanoBioPhotonics (nanofret.com)
Institut d'Electronique Fondamentale
Université Paris-Sud and CNRS
91405 Orsay Cedex (France)
E-mail: niko.hildebrandt@u-psud.fr
Dr. D. Geißler
BAM, Federal Institute for Materials Research and Testing
Division 1.10 Biophotonics
Berlin-Adlershof (Germany)

Supporting information for this article is available on the WWW under http://dx.doi.org/10.1002/anie.201504887.

Table 1: miRNA detection technologies and their performance parameters concerning clinical diagnostics.

	Technology [Refs.][a]	Quantitative	Rapid[b]	Homogeneous[c]	Multiplexed	Const. temp.	High throughput[d]	Liquid-phase kinetics	Amplification free	POCT[e]	Sensitivity
A	Northern blot[9, 25]	√	×	×	×	×	×	×	√	×	−
	Microarray[6, 9, 26, 30]	×	×	×	√	×	√	×	√	×	−
	RT-PCR[6, 9, 25, 26, 30]	√	×	×	√	×	√	√	×	√	++
	Nanostring nCount[30]	√	×	×	√*	×	×	×	√	×	+
	Deep sequencing[6, 9, 30]	×	×	×	√	×	√	×	√	×	++
	Rolling-circle amplification[6, 27]	√	√	×	×	×	×	√	×	√	+
	Electrochemistry[9, 26, 30]	√	×	×	×	√	×	×	√	√	+
	SPR imaging[9, 25]	√	√	×	√*	√	×	×	√	√	+
	Surface-enhanced Raman spectroscopy[9, 26]	√	√	×	√*	√	×	×	√	√	+
	Bioluminescence[9, 25, 26]	√	√	×	×	×	√	×	√	√	+
	Fluorescence correlation spectroscopy[9, 25]	√	×	×	√*	√	×	√	√	×	+
	Fluorescence in situ hybridization[6, 9]	×	×	×	√	×	×	√	√	×	−
	QD-based fluorescence[25, 26, 28]	√	√	×	×	×	×	√	×	√	+
	Time-gated fluorescence[29]	√	√	×	×	√	×	√	√	√	+
B	Time-gated FRET ligation (this work)	√	√	√	√	√	√	√	√	√	+

[a] SPR = surface plasmon resonance, QD = quantum dot. [b] Short measurement times (less than ca. 1 min) and short total assay times including preparation, incubation, and measurement (less than ca. 2 h). [c] Single-step preparation without washing and separation procedures (mix and measure). [d] Tests that use arrays (micro- or nano-) and/or microtiter plates for parallel or serial detection of many samples (e.g. to be applied in clinical laboratories). [e] Point-of-care testing: simple tests with low equipment costs and miniaturization feasibility; √ = available; × = not available; * = single sample (i.e. no parallel detection from several samples such as in microarrays); − = nM to mM; + = fM to nM; ++ = zM to fM.

The extremely long excited-state lifetime of Tb (ca. 2.7 ms) were used for time-gated PL detection, which efficiently suppressed sample background fluorescence and led to highly sensitive detection of miRNA without amplification. Using a versatile assay design (Figure 2), the donor–acceptor distances were optimized for a triplexed signal change in the time window from 0.05 to 0.15 ms. Because freely diffusing Tb and dye oligonucleotides were always present in the assays (homogeneous assay without washing), the addition of low target concentrations led to relatively weak FRET quenching of Tb PL as shown in Figure 1c. However, the dye acceptors were strongly FRET-sensitized as shown in Figure 1d.

The nucleic acid assay was designed to be free of any washing or separation steps and for its application on a clinical fluorescence immunoassay plate reader (KRYPTOR, Cezanne/ThermoFisher). It combines different hybridization and ligation steps for probe–target recognition, which allows the use of a constant and low working temperature ($\leq 37\,^{\circ}C$, insensitive to precursor miRNA interferences) even for RNAs or DNAs with very different melting temperatures (T_m). The hybridization/ligation concept provides maximum selectivity, sensitivity, and versatility for a facile adaption to any short nucleic acid sequence. The working principle is described in Figure 2. The probe is composed of two FRET oligonucleotides (FRET oligos) and two adaptor oligonucleotides (adaptor oligos). The FRET oligos consist of a Tb donor or a dye acceptor, adaptable polynucleotide overhangs (O1 and O2), and a specific hybridization sequence. The adaptor oligos consist of a specific sequence for the donor (FRET-D) or acceptor (FRET-A) probe oligos, and a sequence (TGT-A or TGT-D) that is specific to a part of the target. The assays also contain ligase for the ligation of TGT-D and TGT-A (using ATP in the solution and a 5′-phosphate (P) modification integrated in TGT-A). Mixing of probe and target leads to the formation of stable FRET adaptor oligo double-strands and of semistable adaptor–target complexes with an adaptor nick over the target splint (Figure 2b). Ligation of this nick leads to the formation of stable double-strands (Figure 2c), which allow Tb-to-dye FRET for multiplexed time-gated PL detection of the three miRNAs miRNA-20a, -20b, and -21 (Figure 2d). This two-step target recognition was used to provide high selectivity even for very homologous target sequences such as for miRNA-20a and miRNA-20b (Figure 2e). The separation of FRET and adaptor oligos has the big advantage of "universal" donor or acceptor FRET oligos, which can be used for different targets because the FRET oligo-specific regions of the adaptor oligos are independent from the target-specific regions. Moreover, different lengths of overhangs on the FRET oligos (for an optimization of the FRET distance) can be used for the same adaptor oligos, which is an important aspect for optimizing the probes for the desired targets. Therefore this approach provides much more versatility over direct labeling of the FRET pairs to the adaptor oligos, in particular for multiplexed assay design.

Fluorescent miRNA detection and ligation concepts for enhanced selectivity are not fundamentally new concepts.

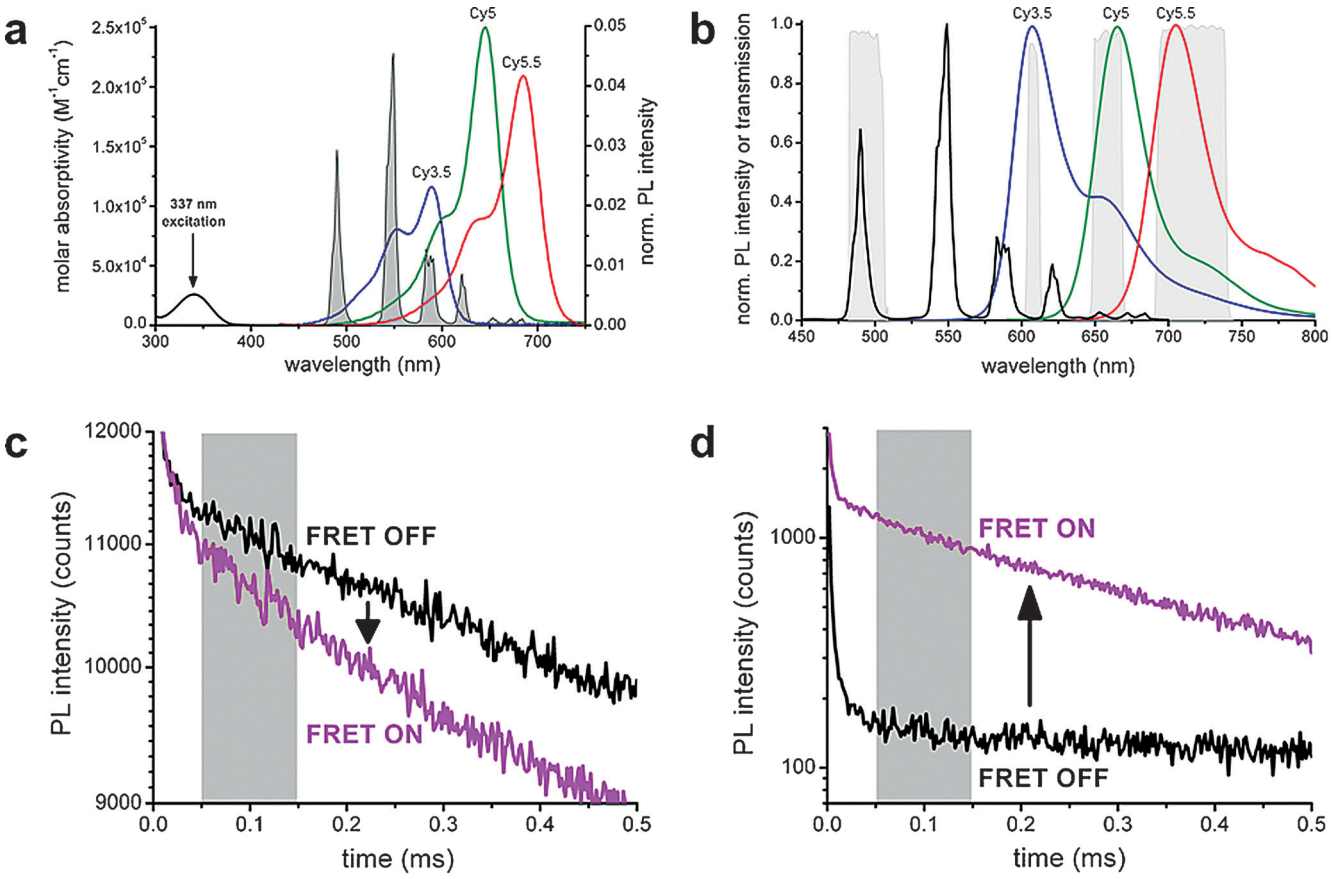

Figure 1. Photophysical properties of the FRET assays. a) Absorbance spectra (left ordinate) of the Tb donor and the acceptor dyes Cy3.5 (blue), Cy5 (green), and Cy5.5 (red). PL spectrum of Tb (gray) is shown for visualization of donor–acceptor spectral overlap. b) PL emission spectra of Tb (black), Cy3.5 (blue), Cy5 (green), and Cy5.5 (red). Transmission spectra of Tb and dye detection channels are show in gray. c,d) Representative PL decay curves measured in the Tb detection channel (c) and in the Cy3.5 detection channel (d) for the Tb-miRNA-20a-Cy3.5 probe. "FRET OFF" curves were detected in the absence of miRNA and represent pure Tb PL. The "FRET ON" curves were detected in the presence of miRNA and represent Tb PL quenching (c) and Cy3.5 PL sensitization (d) due to Tb-to-Cy3.5 FRET. Gray areas represent the time-gated detection windows.

Molecular beacon based fluorescence assays provide very high selectivity due to strand displacement within the loop region by the target. On the other hand, this approach significantly sacrifices sensitivity because an energy barrier (target displacement) must be overcome to open the hairpin. Therefore relatively high target concentrations (low nanomolar range)[19] are required for molecular beacon based assays. However, high sensitivity is a paramount requirement for diagnostics. Reaching lower LODs with molecular beacons can only be achieved by target or signal amplification.[20] Our ligation-based TG-FRET assay was designed to be fully "open" to the target (no target displacement) and can therefore be highly selective (distinction of very homologous targets in a single sample) at ca. 100 to 1000-fold lower concentrations (low picomolar range). Ligation-mediated qRT-PCR techniques (also with fluorescence readout) were shown to provide enhanced selectivity at extremely low concentrations.[21,22] However, these studies did not investigate multiplexed detection and the other disadvantages of qRT-PCR (Table 1) remained unchanged. Therefore our rapid, multiplexed, and highly sensitive FRET assay presents a totally new concept that provides unique advantages and a strong potential for advancing miRNA diagnostics.

To demonstrate the full multiplexing functionality of our assay, we selected the colon adenocarcinoma-relevant miRNAs hsa-miR-20a-5p and hsa-miR-21-5p[23] together with hsa-miR-20b-5p (which is very similar to hsa-miR-20a-5p) as well as their ssDNA analogues (ssDNA-20a/20b/21). The major challenge concerning selectivity was the distinction between miRNA-20a and 20b, whose difference in the RNA sequence can be found in only two out of 23 nucleotides (Figure 2e and Table S1). Such strong sequence homologies are especially difficult to distinguish for homogeneous assays, which do not contain separation, washing, and amplification steps. The probe selectivity was optimized for the detection of miRNA-20a and 20b (Figures S1 and S2a,b) and further verified by using five additional ssDNA targets with very similar sequences to ssDNA20a/b (Figure S2c,d). Although the strongest homology of the miRNA targets was two base-pair mismatches, it can be expected that even single base-pair differences will be distinguishable. As shown in Figure 2d,e the discrimination of miRNA20a and 20b results solely from the TGT-A sequences of the second adaptor oligos (A4a and A4b). The T_m values of these oligos are 30 °C and 20 °C, respectively (Table S1 for 2 mM Mg^{2+} buffer condition). Narrowing down the mismatch to single bases would lead to

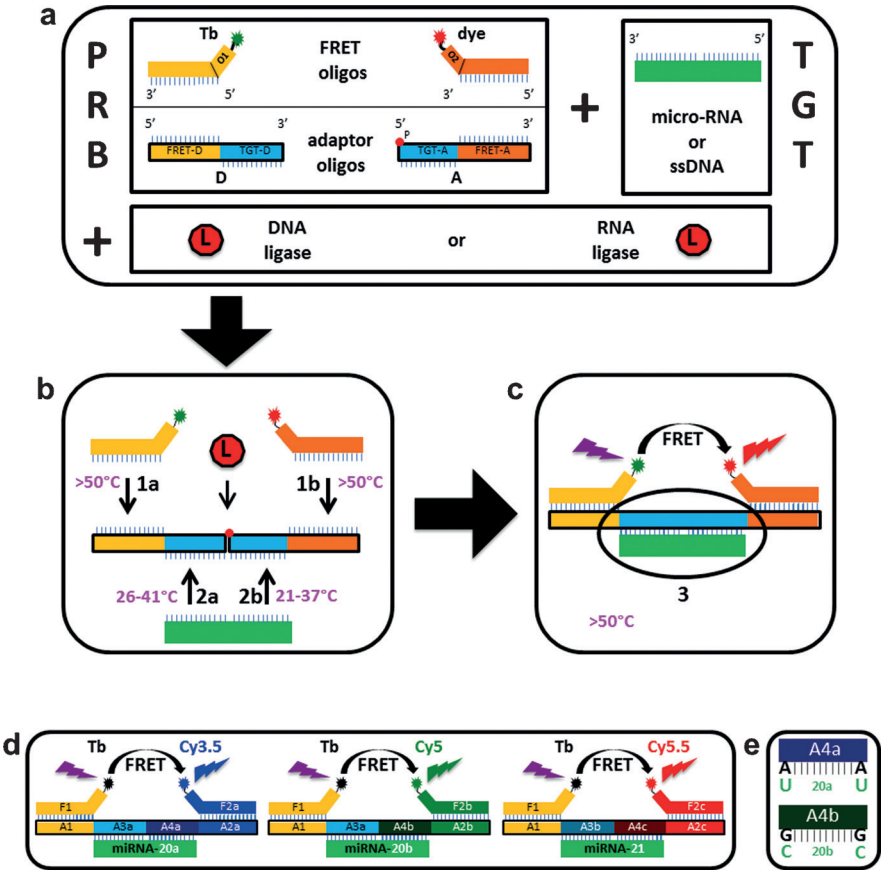

Figure 2. Principle of the multiplexed miRNA FRET assay. a) Each probe (PRB) is composed of two FRET oligos (with adaptable polynucleotide overhangs O1 and O2) and two adaptor oligos. The assays also contain a ligase for the ligation of the adaptor oligos (using ATP in the solution and a 5′-phosphate (P) modification integrated in adaptor oligo A). b) Mixing of probe and target (TGT) leads to the formation of stable FRET–adaptor double-strands (1a and 1b, melting temperatures $T_m > 50\,°C$) and the formation of semistable adaptor–TGT complexes (T_m target- and assay-specific), with an adaptor nick over the TGT splint. Ligation of this nick leads to the formation of stable double-strands. c) Stable PRB–TGT complexes ($T_m > 50\,°C$) allow Tb-to-dye FRET for multiplexed time-gated PL detection of nucleic acid biomarkers. d) FRET assays for triplexed miRNA detection. Labels on the different oligo parts (F: FRET oligo, A: adaptor oligo) describe the persistent or changing parts of the different PRB–TGT complexes (A4a, A4b, A4c, and A3b are RNA, all other parts are DNA). e) Magnification of the different bases in A4a-miRNA-20a and A4b-miRNA-20b base pairing.

an estimated T_m difference of 5 °C, which should still allow an efficient discrimination, in particular when combined with careful positioning of the nick.

One of the main goals of our study was multiplexed detection of several miRNAs or ssDNAs from a single low-volume sample. To demonstrate this, we designed our probes for triplexed assays of miRNA-20a, miRNA-20b, and miRNA-21 (Figure 2d) or their ssDNA analogues, performed on the KRYPTOR plate reader. Because binding of miRNA-20a targets to the Tb-miRNA-20b-Cy5 probes generated biological crosstalk, we adapted the spectral crosstalk correction method for immunoassays[18] to an efficient biospectral crosstalk correction for miRNA diagnostics (see the Supporting Information). Although strong biospectral crosstalk was present in our homogeneous miRNA assays, the upgraded method provided very efficient correction for all three targets (Figure S3), even under complex conditions when the other two targets were present at high and low, low and high, or high and high concentrations (Figures S4 and S5). For a more condensed presentation of the ability to precisely measure very low concentrations of the three targets at different concentrations we prepared nine samples with target concentrations between 0.05 and 0.5 nM and measured these with our homogeneous multiplexed FRET assays using the calibration curves from Figure S3. The results (Figure 3a for miRNA and Figure S6 for ssDNA) provide an impressive demonstration of the extremely high specificity and sensitivity of our one-step miRNA and ssDNA assays even when all three targets are present in the same sample atdifferent concentrations. To demonstrate high precision for a single measurement (2.5 s per measurement), each sample was prepared and measured only once. The error bars present the errors from biospectral crosstalk correction. These assays present measurements in a reduced linear dynamic range (0.05 to 0.75 nM), which actually extends from ca. 0.03 nM (the limit of detection) to ca. 3 nM (the probe concentration), after which the addition of further targets does not lead to any further FRET pairs (saturation of probes). In an automated diagnostic assay this linear range can be increased to higher concentrations by dilution of highly concentrated samples, which are automatically detected by the KRYPTOR plate reader system using kinetic measurements in the very beginning of probe–target incubation.

To demonstrate point-of-care testing (POCT) capability we challenged our assay with direct miRNA detection in a few microliters of serum. Figure 3b–d show the excellent performance for the detection of the three different targets. Although further optimization steps can most probably lead to even higher selectivity and sensitivity our serum-based assays demonstrate the feasibility of a homogeneous multiplexed miRNA and ssDNA detection directly in serum. For the determination of the limits of detection (LOD, zero-concentration value plus three times its standard deviation) of the buffer and serum-based assays under the different conditions we used the various calibration curves and calculated the standard deviation values of 10 zero-concentration samples. Our assays accomplished very low LODs below 0.032 and 0.052 nM (5 and 8 fmol) for miRNA and ssDNA, respectively, in buffer and below 0.9 and 2.0 nM (7 and 15 fmol) for miRNA and ssDNA, respectively, in serum (Table 2).

Table 2: LODs of the different miRNA and ssDNA targets under different sample conditions (in the absence and in the presence of other targets inside the sample).

Target:	miRNA-20a	miRNA-20b	miRNA21	ssDNA-20a	ssDNA-20b	ssDNA-21
Conditions[a]	LOD in 150 μL buffer-based sample [pM]					
X	23	23	21	11	17	25
X + (750 pM Y)	37	29	29	19	29	57
X + (750 pM Z)	36	29	27	15	21	40
X + (750 pM Y and Z)	31	17	23	15	27	86
average	32	24	25	15	23	52
Conditions[a]	LOD in 7.5 μL serum [pM]					
X	230	210	250	390	460	610
X + (750 pM Y)	150	250	700	420	450	1900
X + (750 pM Z)	210	1070	740	400	810	1720
X + (750 pM Y and Z)	200	410	1840	470	490	3680
average	200	490	880	420	550	1980

[a] If X = 20a then Y = 20b and Z = 21; if X = 20b then Y = 21 and Z = 20a; if X = 21 then Y = 20b and Z = 20a.

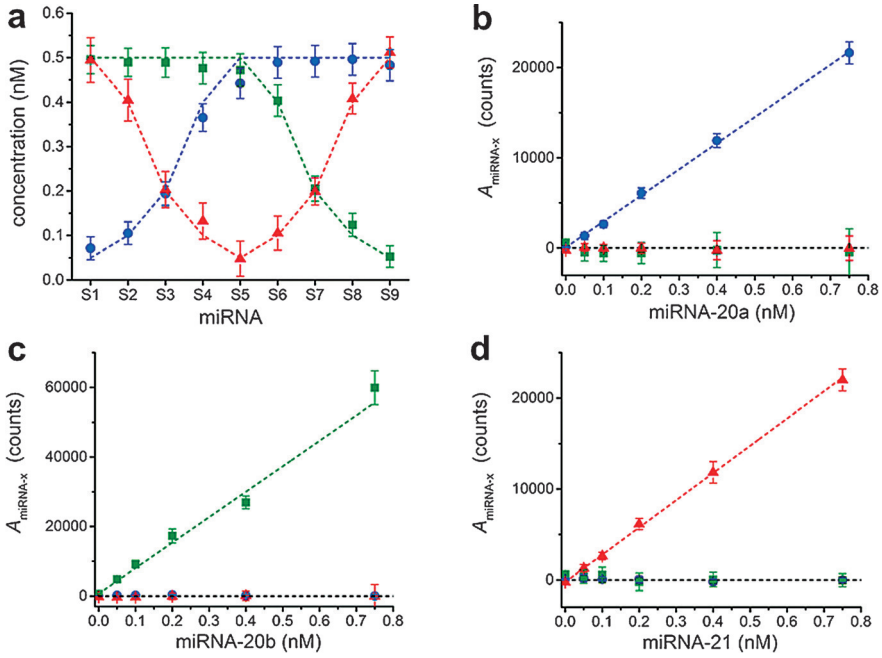

Figure 3. Multiplexed detection of varying miRNA concentrations and miRNA detection directly in serum. a) Nine samples (S1 to S9) containing varying amounts of miRNAs (dotted lines indicate the known concentrations) were measured. Deviations from the dotted lines are due to experimental errors (pipetting and/or excitation intensity). b–d) Calibration curves showing the target-specific signal intensities after biospectral crosstalk correction ($A_{miRNA-x}$) for the targets miRNA-20a (b), miRNA-20b (c,) and miRNA-21 (d) in 7.5 μL serum samples. All assays contain all three probes but only one target per assay. Results for ssDNA can be found in Figure S6. Blue: miRNA-20a; green: miRNA-20b, red: miRNA-21.

Taking into account our previous results in the highly sensitive multiplexed detection of protein biomarkers[18,24] and the versatility of the assay design it can be expected that our technology will be adaptable to higher-order multiplexing and lower LODs and can be transferred to any short nucleic acid sequence with a length between roughly 10 and 26 nucleotides. Therefore our homogeneous multiplexed FRET assay will most probably also find application in other important types of nucleic acid analysis, such as genetic variation of mRNA for inherited diseases, drug resistance during cancer treatment, single-stranded viral RNA or DNA due to viral infections, and in fluorescence imaging of in vitro cultured cells and fixed or fresh-frozen tissue samples to uncover the molecular basis and pathological evolution of many different diseases.

Acknowledgements

We thank Lumiphore, Inc. for the gift of Lumi4 reagents and Honghua Quan for technical assistance. This work was supported by the European Commission (Innovative Medicine Initiative project OncoTrack), the Agence Nationale de la Recherche France (project NanoFRET), and the Chinese Scholarship Council. Université Paris-Sud, CNRS, and Lumiphore have filed a provisional patent application, EP14305794.1, on the described method of multiplexed homogeneous oligonucleotide detection.

Keywords: clinical diagnostics · FRET · microRNA · multiplexing · time-gated fluorescence detection

How to cite: *Angew. Chem. Int. Ed.* **2015**, *54*, 10024–10029
Angew. Chem. **2015**, *127*, 10162–10167

[1] D. P. Bartel, *Cell* **2009**, *136*, 215–233.
[2] S. L. Ameres, M. D. Horwich, J. H. Hung, J. Xu, M. Ghildiyal, Z. Weng, P. D. Zamore, *Science* **2010**, *328*, 1534–1539.
[3] S. L. Ameres, P. D. Zamore, *Nat. Rev. Mol. Cell Biol.* **2013**, *14*, 475–488.
[4] A. E. Frampton, T. M. Gall, L. Castellano, J Stebbing, L. R. Jiao, J. Krell, *Expert Rev. Mol. Diagn.* **2013**, *13*, 31–34.

[5] H. Schwarzenbach, K. Pantel, *MicroRNAs in Medicine*, 1st ed., Wiley, Hoboken, **2014**, pp. 567 – 588, ISBN: 9781118300398.
[6] M. de Planell-Saguer, M. C. Rodicio, *Clin. Biochem.* **2013**, *46*, 869 – 878.
[7] M. V. Iorio, C. M. Croce, *EMBO Mol. Med.* **2012**, *4*, 143 – 159.
[8] R. Ma, T. Jiang, X. Kang, *J. Exp. Clin. Cancer Res.* **2012**, *31*, 38.
[9] M. de Planell-Saguer, M. C. Rodicio, *Anal. Chim. Acta* **2011**, *699*, 134 – 152.
[10] Z. Gao, H. Deng, W. Shen, Y. Ren, *Anal. Chem.* **2013**, *85*, 1624 – 1630.
[11] Y. Ren, H. Deng, W. Shen, Z. Gao, *Anal. Chem.* **2013**, *85*, 4784 – 4789.
[12] R. Redon, S. Ishikawa, K. R. Fitch, L. Feuk, G. H. Perry, T. D. Andrews, H. Fiegler, M. H. Shapero, A. R. Carson, W. Chen, E. K. Cho, S. Dallaire, J. L. Freeman, J. R. González, M. Gratacòs, J. Huang, D. Kalaitzopoulos, D. Komura, J. R. MacDonald, C. R. Marshall, R. Mei, L. Montgomery, K. Nishimura, K. Okamura, F. Shen, M. J. Somerville, J. Tchinda, A. Valsesia, C. Woodwark, F. Yang, J. Zhang, T. Zerjal, J. Zhang, L. Armengol, D. F. Conrad, X. Estivill, C. Tyler-Smith, N. P. Carter, H. Aburatani, C. Lee, K. W. Jones, S. W. Scherer, M. E. Hurles, et al., *Nature* **2006**, *444*, 444 – 454.
[13] H. Okamoto, Y. Sugiyama, S. Okada, K. Kurai, Y. Akahane, Y. Sugai, T. Tanaka, K. Sato, F. Tsuda, Y. Miyakawa, M. Mayumi, *J. Gen. Virol.* **1992**, *73*, 673 – 679.
[14] Y.-L. Wei, C.-X. Li, J. Jia, L. Hu, Y. Liu, *J. Forensic Sci.* **2012**, *57*, 1448 – 1456.
[15] G. G. Fortes, C. F. Speller, M. Hofreiter, T. E. King, *Bioassays* **2013**, *35*, 690 – 695.
[16] N. Hildebrandt, K. D. Wegner, W. R. Algar, *Coord. Chem. Rev.* **2014**, *125*, 273 – 274.
[17] J. Xu, T. M. Corneillie, E. G. Moore, G.-L. Law, N. G. Butlin, K. N. Raymond, *J. Am. Chem. Soc.* **2011**, *133*, 19900 – 19910.
[18] D. Geißler, S. Stufler, H.-G. Löhmannsröben, N. Hildebrandt, *J. Am. Chem. Soc.* **2013**, *135*, 1102 – 1109.
[19] M. B. Baker, G. Bao, C. D. Searles, *Nucleic Acids Res.* **2012**, *40*, e13.
[20] J. Lu, A. Tsurkas, *Nucleic Acids Res.* **2009**, *37*, e100.
[21] Y. Q. Du, P. F. Gao, W. Wang, T. T. Wang, Y. Chang, J. Wang, C. Z. Huang, *Analyst* **2013**, *138*, 5745 – 5750.
[22] J. Zhang, Z. Li, H. Wang, H. Jia, J. Yan, *Chem. Commun.* **2011**, *47*, 9465 – 9467.
[23] A. J. Schetter, S. Y. Leung, J. J. Sohn, K. A. Zanetti, E. D. Bowman, N. Yanaihara, S. T. Yuen, T. L. Chan, D. L. Kwong, G. K. Au, C. G. Liu, G. A. Calin, C. M. Croce, C. C. Harris, *JAMA J. Am. Med. Assoc.* **2008**, *299*, 425.
[24] D. Geißler, L. J. Charbonnière, R. F. Ziessel, N. G. Butlin, H. G. Löhmannsröben, N. Hildebrandt, *Angew. Chem. Int. Ed.* **2010**, *49*, 1396 – 1401; *Angew. Chem.* **2010**, *122*, 1438 – 1443.
[25] K. A. Cissell, Y. Rahimi, S. Shrestha, E. A. Hunt, S. K. Deo, *Anal. Chem.* **2008**, *80*, 2319 – 2325.
[26] H. Zhang, Y. Liu, X. Fu, L. Yuan, Z. Zhu, *Microchim. Acta* **2015**, *182*, 661 – 669.
[27] Y. Cheng, X. Zhang, Z. Li, X. Jiao, Y. Wang, Y. Zhang, *Angew. Chem. Int. Ed.* **2009**, *48*, 3268 – 3272; *Angew. Chem.* **2009**, *121*, 3318 – 3322.
[28] A. Fang-ju Jou, C.-H. Lu, Y.-C. Ou, S.-S. Wang, S.-L. Hsu, I. Willner, J.-A. Annie Ho, *Chem. Sci.* **2015**, *6*, 659 – 665.
[29] L. Jiang, D. Duan, Y. Shen, J. Li, *Biosens. Bioelectron.* **2012**, *34*, 291 – 295.
[30] P. Mestdagh, N. Hartmann, L. Baeriswyl, D. Andreasen, N. Bernard, C. Chen, D. Cheo, P. D'Andrade, M. DeMayo, L. Dennis, S. Derveaux, Y. Feng, S. Fulmer-Smentek, B. Gerstmayer, J. Gouffon, C. Grimley, E. Lader, K. Y. Lee, S. Luo, P. Mouritzen, A. Narayanan, S. Patel, S. Peiffer, S. Rüberg, G. Schroth, D. Schuster, J. M. Shaffer, E. J. Shelton, S. Silveria, U. Ulmanella, V. Veeramachaneni, F. Staedtler, T. Peters, T. Guettouche, L. Wong, J. Vandesompele, *Nat. Methods* **2014**, *11*, 809 – 815.

Received: May 29, 2015
Published online: July 29, 2015

